proposed antenna is an attractive candidate for wireless communications.

REFERENCES

1. J.S. Row and J.F. Wu, Aperture-coupled microstrip antenna with switchable polarization, IEEE Trans Antennas Propag 54 (2006), 2686–2691.
2. K. Chung, Y. Nam, T. Yun, and J. Choi, Reconfigurable microstrip patch antenna with frequency and polarization diversity functions, Microwave Opt Technol Lett 47 (2005), 605–607.
3. M.-H. Ho, M.-T. Wu, C.-I.G. Hsu, and J.-Y. Sze, An RHCP/LHCP switchable slotline-fed ring-slot antenna, Microwave Opt Technol Lett 46 (2005), 30–33.
4. Y.B. Chen, Y.C. Jiao, and F.S. Zhang, Polarization reconfigurable cpw-fed square slot antenna using pin diodes, Microwave Opt Technol Lett 49 (2007), 1233–1236.
5. J. Ouyang, F. Yang, and S. Yang, A novel reconfigurable circular polarization patch antenna, Microwave Opt Technol Lett 50 (2008), 1921–1923.
6. K. Chung, Y. Nam, T. Yun, and J. Choi, Reconfiguralbe microstrip-patch antenna with frequency and polarization-diversity functions, Microwave Opt Technol Lett 47 (2005), 605–607.
7. C.-H. Hu, T.-R. Chen, J.-F. Wu, and J.-S. Row, Reconfigurable microstrip antenna with polarisation diversity and frequency agility, Electron Lett 43 (2007).
8. J.-F. Wu, J.-S. Row, and K.-L. Wong, Dual-frequency circularly-polarized microstrip antenna with switchable polarization sense, Microwave Opt Technol Lett 50 (2008), 2125–2128.
9. K.-L. Wong, C.-C. Huang, and W.-S. Chen, Prented ring slot antenna for circular polarization, IEEE Trans Antennas Propag 50 (2002), 75–77.
10. F. Yang and Y. Rahmat-Samii, Patch antenna with switchable slot (PASS): Dual-frequency operation, Microwave Opt Technol Lett 31 (2001), 165–168.

SEVEN-BAND FOLDED-LOOP CHIP ANTENNA FOR WWAN/WLAN/WiMAX OPERATION IN THE MOBILE PHONE

Ming-Ren Hsu and Kin-Lu Wong
Department of Electrical Engineering, National Sun Yat-Sen University, Kaohsiung 804, Taiwan; Corresponding author: hsumr@ema.ee.nsysu.edu.tw

Received 3 June 2008

ABSTRACT: *A chip antenna formed by using an FR4 chip base and a folded-loop metal pattern embedded therein for internal mobile phone antenna application is presented. The folded-loop metal pattern is embedded in two different layers inside the FR4 chip base to achieve a compact structure, and a coupling gap is introduced to successfully excite two wide operating bands at about 900 and 2000 MHz to cover GSM850/900/1800/1900/UMTS, 2.4-GHz WLAN, and 2.5-GHz WiMAX operations; that is, a seven-band internal mobile phone antenna for covering WWAN/WLAN/WiMAX operation is obtained. The proposed chip antenna also occupies a small volume of 4 × 5 × 40 mm³ (0.8 cm³) and shows a low profile of 5 mm when mounted on the system circuit board of the mobile phone, making it suitable for thin mobile phone applications. The proposed chip antenna is studied and tested. The SAR effect of the antenna is also analyzed in the study.* © 2008 Wiley Periodicals, Inc. Microwave Opt Technol Lett 51: 543–549, 2009; Published online in Wiley InterScience (www.interscience.wiley.com). DOI 10.1002/mop.24063

Key words: *chip antennas; internal mobile phone antennas; loop antennas; seven-band operation; multiband operation*

1. INTRODUCTION

It has recently been shown that the loop antenna is very promising for internal mobile phone antenna applications. Many promising internal multiband loop antennas have been reported [1–8]. These available loop antennas are fabricated from bending the metal strip/wire or printing on a supporting dielectric substrate [1–5], printing directly on the system circuit board of the mobile phone [6, 7], or mounting the loop metal pattern on a foam base as a surface-mount element [8]. In this article, we report another promising and compact multiband loop antenna as a surface-mount element for mobile phone application. The loop metal pattern is folded and embedded in two different layers inside a small FR4 chip base of $4 \times 5 \times 40$ mm^3 (0.8 cm^3) to achieve a compact structure. By further introducing a coupling gap along the loop metal pattern near the feeding point of the antenna, two wide operating bands at about 900 and 2000 MHz can be obtained. The lower band at about 900 MHz can easily cover GSM850/900 (824–894/890–960 MHz) operation. The upper band at about 2000 MHz can cover not only GSM1800/1900/UMTS (1710–1880/1850–1990/1920–2170 MHz) operation but also WLAN operation in the 2.4-GHz band (2400–2484 MHz) and WiMAX operation in the 2.5-GHz band (2500–2690 MHz). That is, the proposed folded-loop chip antenna can cover seven-band operation for wireless wide area network (WWAN), wireless local area network (WLAN) [9], and worldwide interoperability for microwave access (WiMAX) [10, 11] operation, providing voice and seamless wireless internet access for wireless users.

The proposed chip antenna also shows a low profile of 5 mm only when mounted on the system circuit board of the mobile phone. The low profile is attractive for thin mobile phone applications [12, 13]. Details of the proposed chip antenna are described, and results of the fabricated prototype are presented and discussed. The specific absorption rate (SAR) [14–16] effect for the proposed antenna mounted at the top and bottom positions of the system circuit board of the mobile phone is also analyzed.

2. PROPOSED FOLDED-LOOP CHIP ANTENNA

Figure 1(a) shows the geometry of the proposed folded-loop chip antenna mounted at the top edge of the no-ground portion (10×40 mm^2) of the system circuit board (110×40 mm^2) of the mobile phone. The system circuit board is a 0.8-mm thick FR4 substrate used in the study; on the back side of the system circuit board, there is a printed ground plane of 100×40 mm^2 as the system ground plane. A 1-mm thick plastic housing of relative permittivity 3.0 and loss tangent 0.02 treated as the casing of the practical mobile phone is used in the study. The FR4 chip base of relative permittivity 4.4, loss tangent 0.0245, and volume $4 \times 5 \times 40$ mm^3 is used for the antenna. The folded-loop metal pattern is formed on two different layers inside the FR4 chip base; dimensions of the unfolded metal pattern are shown in Figure 1(b). The two layers are layers 1 and 2 with a spacing of 0.8 mm in between, and the total thickness of the FR4 chip base is 4 mm. Layers 1 and 2 are connected through two via-holes at points E and F; in this case, a loop metal pattern between soldering points C and D is formed. Also note that points C and D are located on the bottom surface of the FR4 chip base; point C is connected to the feeding metal strip and point D is connected to the grounding metal strip, both of length 8.4 mm and width 1.5 mm and printed on the no-ground portion of the system circuit board. The feeding metal strip is further connected at point A to a 50-Ω microstrip feedline printed

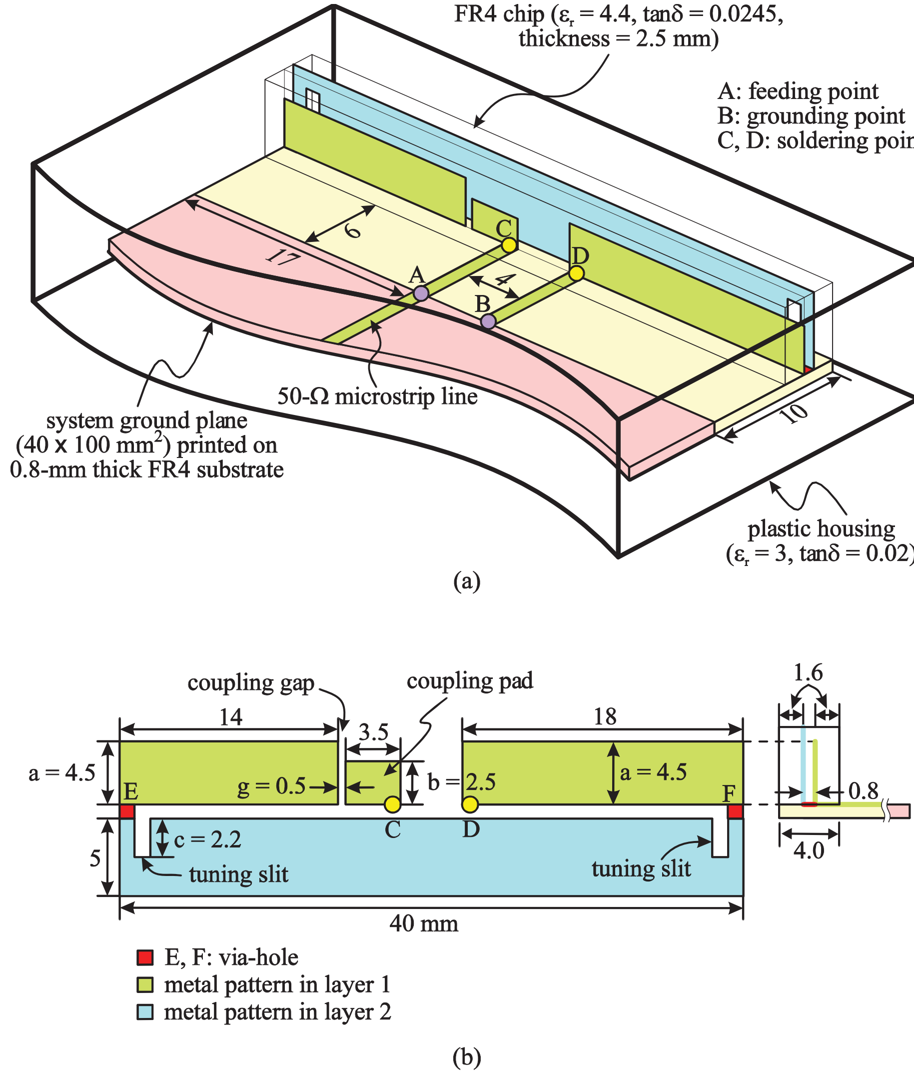

Figure 1 (a) Geometry of the seven-band folded-loop chip antenna for WWAN/WLAN/WiMAX operation in the mobile phone; the antenna is enclosed by a 1-mm thick plastic housing. (b) Dimensions of the metal pattern inside the chip antenna in its unfolded structure. [Color figure can be viewed in the online issue, which is available at www.interscience.wiley.com]

on the front side of the system circuit board for testing the antenna in the study. The grounding metal strip is grounded at point B through a via-hole to the top edge of the system ground plane on the back side of the system circuit board.

In layer 1, a coupling gap of 0.5 mm is introduced near point C, separating the left-hand side metal portion of layer 1 into a small rectangular coupling pad of width (b) 2.5 mm and length 3.5 mm connected to the soldering point C and a radiating portion connected to the via-hole at point E. By adjusting the width b of the coupling pad in the proposed design, some additional capacitance can be contributed to the antenna's input impedance, which is found to result in decreased impedance variations for frequencies over the desired operating bands. Hence, wider operating bands for covering the desired WWAN/WLAN/WiMAX operation can be achieved.

The total length of the folded-loop metal pattern embedded inside the FR4 chip base and the two printed metal strips on the no-ground portion reaches about 100 mm, which supports a 0.5-wavelength loop resonant mode at about 900 MHz for the antenna's lower band to cover GSM850/900 operation. In addition, several higher-order loop resonant modes are also excited with good impedance matching to form a very wide operating band as the antenna's upper band to cover GSM1800/1900/UMTS/WLAN/WiMAX operation.

It is also noted that by adjusting the width a of the radiating portion in layer 1, the lower-edge frequency of the antenna's upper band can be adjusted to be less than 1710 MHz to cover GSM1800 operation. In addition, there are two tuning slits of length (c) 2.2 mm introduced in layer 2 to help adjust the impedance matching for frequencies over the antenna's lower and upper bands. Detailed effects of the tuning parameters in the proposed design such as the width a of the radiating portion in layer 1, the width b of the coupling pad in layer 1, and the length c of the tuning slits in layer 2 on the antenna performance will be discussed in the next section.

3. RESULTS AND DISCUSSION

A prototype of the proposed antenna with dimensions given in Figure 1 was constructed and tested. Figure 2 shows the measured and simulated return loss for the constructed antenna. The simulated results are obtained using Ansoft HFSS [17], and an agreement between the measurement and simulation is observed. With the definition of 3:1 VSWR (6-dB return loss) generally used for internal mobile phone antenna design, the generated lower band

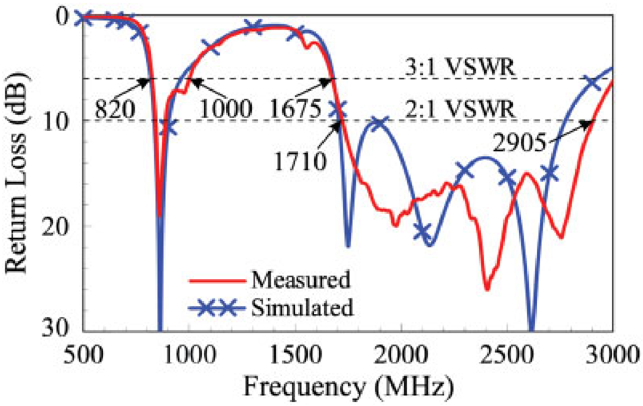

Figure 2 Measured and simulated return loss for the proposed antenna. [Color figure can be viewed in the online issue, which is available at www.interscience.wiley.com]

shows an impedance bandwidth of 180 MHz (820–1000 MHz), allowing the antenna to easily cover GSM850/900 operation. The obtained upper band shows a much wider impedance bandwidth (larger than 1 GHz). For frequencies over the GSM1800/1900/UMTS bands, the impedance matching is better than not only 3:1 VSWR but also 2:1 VSWR (9.6-dB return loss). The upper band also covers the 2.4-GHz WLAN and the 2.5-GHz WiMAX bands, with the impedance matching better than 2:1 VSWR.

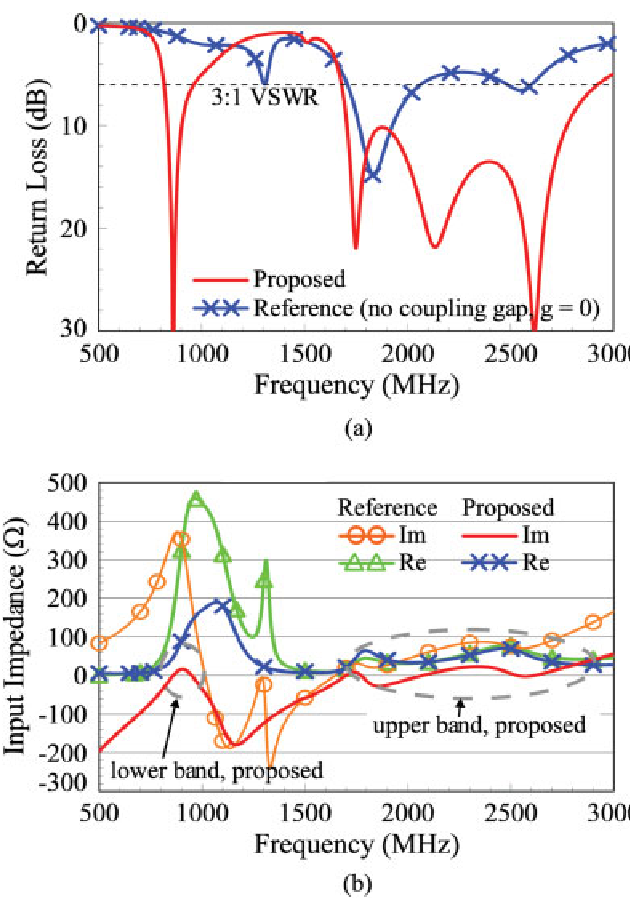

Figure 3 Simulated (a) return loss and (b) input impedance of the proposed and reference antennas. [Color figure can be viewed in the online issue, which is available at www.interscience.wiley.com]

Figure 3 shows the simulated return loss and input impedance of the proposed and reference antennas; the reference antenna is for the case of no coupling gap ($g = 0$) in the proposed design in Figure 1. It can be seen that in Figure 3(a), owing to the presence of the coupling gap, much improved impedance matching for frequencies over the desired antenna's lower and upper bands is obtained for the proposed antenna. This can be seen more clearly for the input impedance results shown in Figure 3(b). At around 900 MHz for the reference antenna, there are large variations in the input impedance curve. While for the proposed antenna, the real part (Re curve) of the input impedance is greatly decreased and the imaginary part (Im curve) is also greatly compensated by the contributed capacitance from the coupling gap, hence resulting in the successful excitation of a wide operating band at about 900 MHz for covering GSM850/900 operation. For frequencies over the desired upper band, similar behavior is also observed, leading to a very wide operating band of larger than 1 GHz obtained for covering GSM1800/1900/UMTS/WLAN/WiMAX operation.

Figures 4–6 show the parametric study of the proposed antenna. Figure 4 demonstrates the simulated return loss of the width a of the radiating portion in layer 1 of the proposed antenna. When the width a is varied from 4.0 to 5.0 mm, only the lower-edge frequency of the antenna's upper band is decreased, with the antenna's fundamental resonant mode (0.5-wavelength loop resonant mode) at about 900 MHz and other resonant modes in the upper band very slightly affected. This indicates that the lower-edge frequency of the antenna's upper band can be generally be controlled separately by adjusting the width a of the radiating portion in layer 1 of the proposed antenna.

Figure 5 shows the simulated return loss of the width b of the coupling pad in layer 1 of the proposed antenna. By adjusting the width b from 2.0 to 3.0 mm, the impedance matching for frequencies over the antenna's lower and upper bands is varied. That is mainly because the coupling pad controls the contributed capacitance to the input impedance of the antenna. Figure 6 shows the simulated return loss of the length c of the tuning slits in layer 2 of the proposed antenna. When the length c of the tuning slits is varied from 1.7 to 2.7 mm, the antenna's fundamental resonant

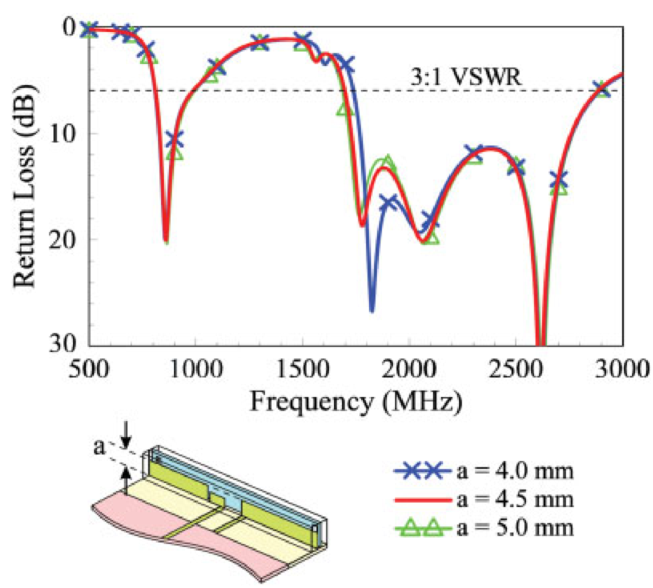

Figure 4 Simulated return loss as a function of the width a of the radiating portion in layer 1 of the proposed antenna. [Color figure can be viewed in the online issue, which is available at www.interscience.wiley.com]

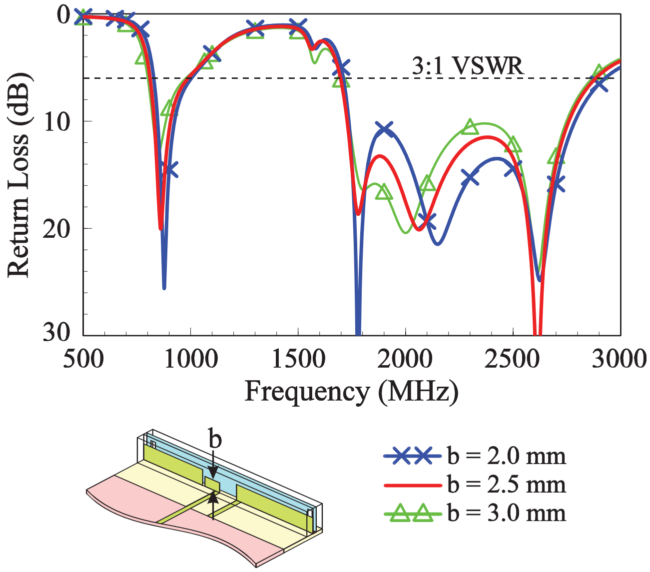

Figure 5 Simulated return loss as a function of the width *b* of the coupling pad in layer 1 of the proposed antenna. [Color figure can be viewed in the online issue, which is available at www.interscience.wiley.com]

mode in the lower band and the lower-edge frequency of the antenna's upper band are both shifted toward lower frequencies. This can be attributed to the effective resonant loop path of the proposed antenna being lengthened by increasing the length of the tuning slits. Hence, by adjusting the parameters of *a, b,* and *c* in the proposed design, good impedance matching for frequencies over the antenna's desired lower and upper bands can be obtained.

Radiation characteristics of the constructed prototype are also studied. Figure 7 plots the measured radiation patterns at 859 and 925 MHz, the central frequencies of the GSM850 and GSM900 bands. Monopole-like radiation patterns are observed, which is similar to those of the conventional internal mobile phone antennas

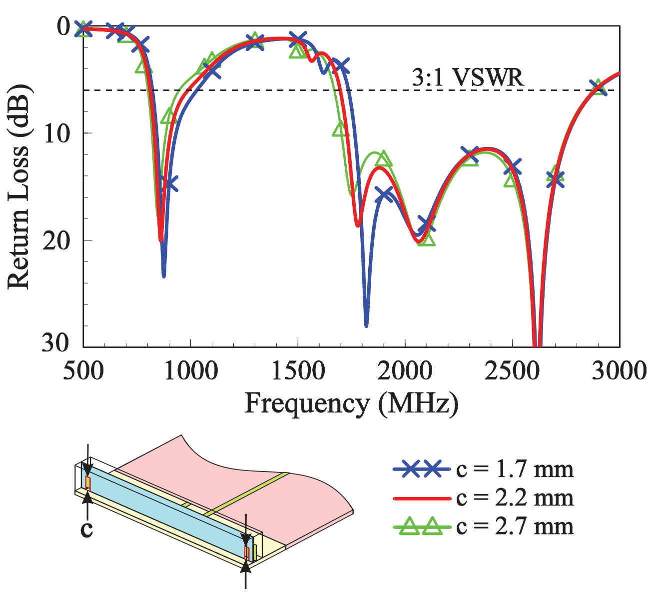

Figure 6 Simulated return loss as a function of the length *c* of the tuning slits in layer 2 of the proposed antenna. [Color figure can be viewed in the online issue, which is available at www.interscience.wiley.com]

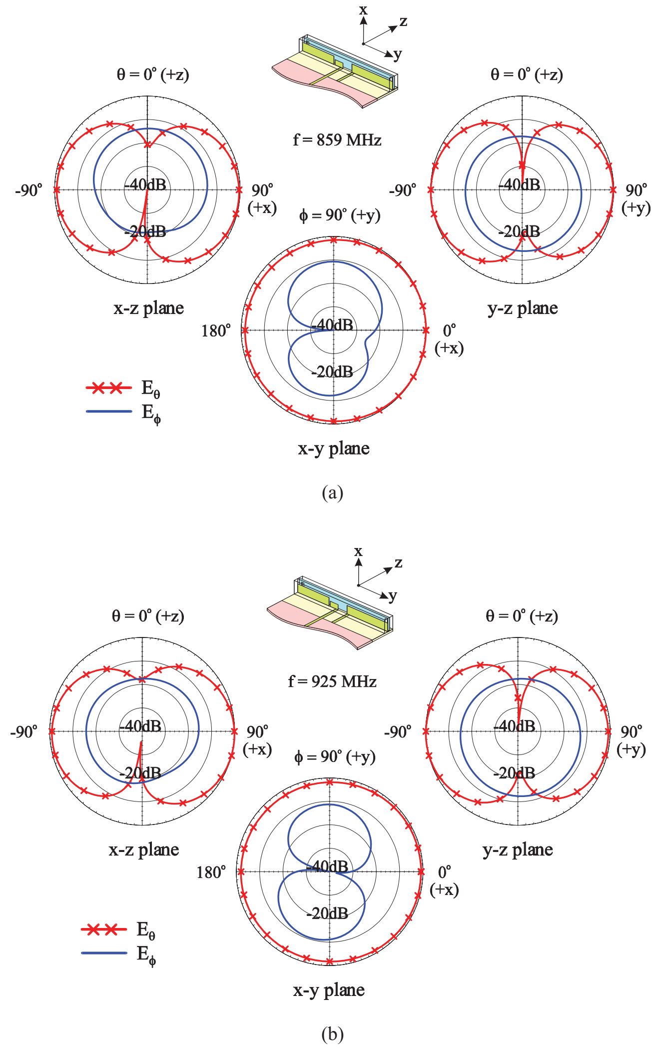

Figure 7 Measured radiation pattern for the proposed antenna. (a) 859 MHz; (b) 925 MHz. [Color figure can be viewed in the online issue, which is available at www.interscience.wiley.com]

for GSM operation. Figure 8 plots the measured radiation patterns at 1795, 1920, and 2045 MHz, the central frequencies of the GSM1800, GSM1900, and UMTS bands. The measured radiation patterns show no special distinctions as compared to those of the conventional internal mobile phone antennas operated at the corresponding frequencies. Figure 9 plots the measured radiation patterns at 2450 and 2600 MHz, about the central frequencies of the WLAN and WiMAX bands. Comparable E_θ and E_ϕ components are generally observed, which is advantageous since the wave propagation environment is usually complex for practical applications.

Figure 10 shows the measured antenna gain and the simulated radiation efficiency of the constructed prototype. Over the GSM850/900 band shown in Figure 10(a), the antenna gain is varied from about −0.3 to 1.1 dBi, and the radiation efficiency is varied from about 55% to 77%. Over the GSM1800/1900/UMTS band shown in Figure 10(b), the antenna gain ranges from about 0.8 to 3.2 dBi, and the radiation efficiency is varied from about 50% to 93%. Over the WLAN/WiMAX band, the antenna gain varies from about 3.2 to 4.2 dBi, and a stable radiation efficiency of about 92% is obtained.

Figure 11 shows the SAR simulation model for the antenna at the top and bottom positions with the head phantom provided by

SEMCAD [18, 19], and the simulated SAR results are also given. Note that for operating in the lower band, the maximum transmitted power is 33 dBm, with a 1/8 time slot used; this means that the incident power is 24 dBm in the lower band. It is observed that the SAR values at 1 g tissue with the antenna at the top and bottom

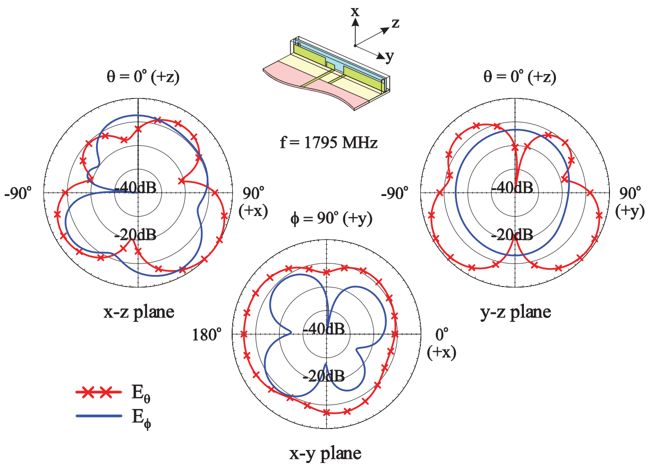

(a)

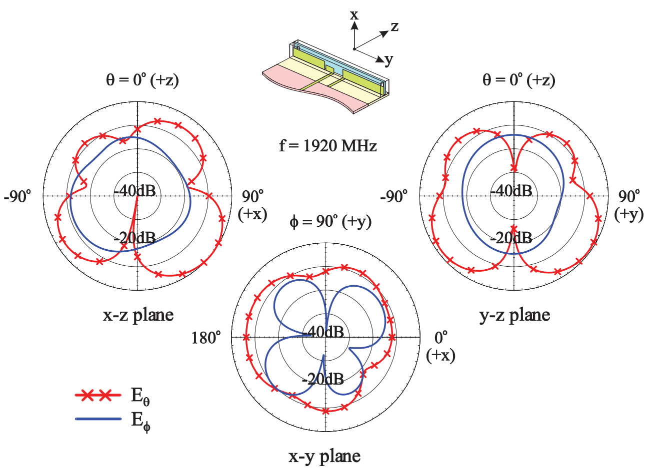

(b)

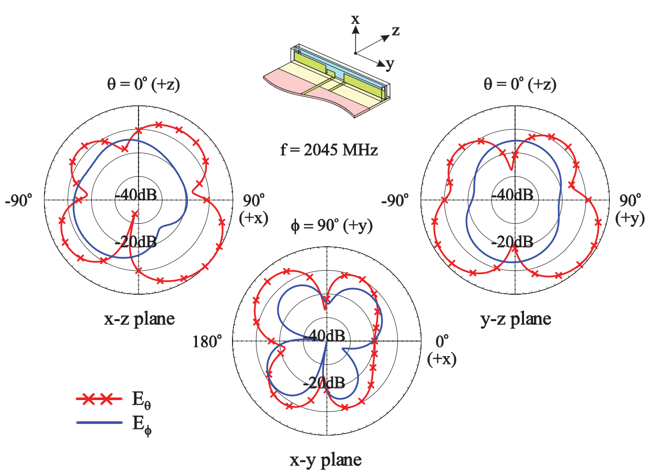

(c)

Figure 8 Measured radiation pattern for the proposed antenna. (a) 1795 MHz; (b) 1920 MHz; (c) 2045 MHz. [Color figure can be viewed in the online issue, which is available at www.interscience.wiley.com]

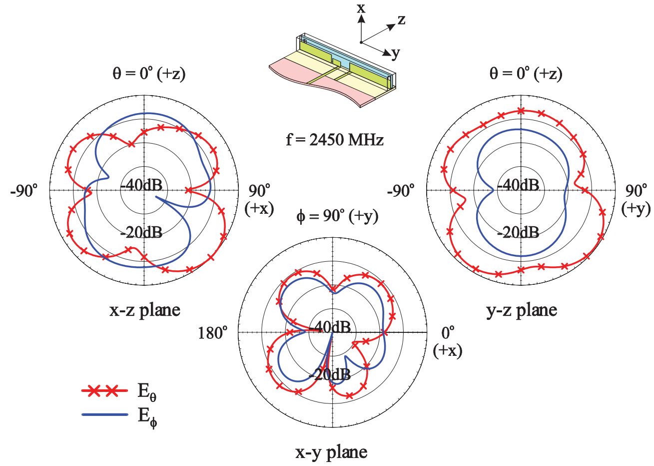

(a)

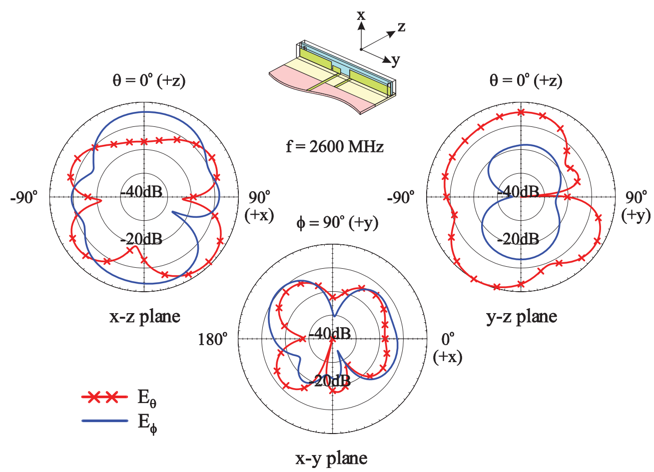

(b)

Figure 9 Measured radiation pattern for the proposed antenna. (a) 2450 MHz. (b) 2600 MHz. [Color figure can be viewed in the online issue, which is available at www.interscience.wiley.com]

positions of the mobile phone are 2.10 and 1.68 W/kg, respectively; that is, the SAR decrease in decibels for the antenna at the bottom position to that at the top position is about 0.96 dB. For operating in the upper band, the maximum transmitted power is 30 dBm, indicating that the incident power with the 1/8 time slot considered is 21 dBm. The simulated result shows that the SAR values at 1-g tissue with the antenna at the top and bottom positions of the mobile phone are 2.49 and 1.23 W/kg, respectively. This indicates a SAR decrease of about 3.08 dB for the antenna at the bottom position to that at the top position. These SAR results can be explained from the simulated SAR distributions shown in Figure 12. For the antenna at the top position [see Fig. 12(a)], the hot spot (local maximum SAR) appears near the user's ear at 925 MHz. While for the antenna at the bottom position at 925 MHz [see Fig. 12(b)], the hot spot is shifted toward the user's cheek and is with a decreasing value. This explains the SAR decrease at 925 MHz indicated in Figure 11. For operating at 1920 MHz, the hot spot for the antenna at the top and bottom positions are both near the user's ear; however, the hot spot is with a much smaller SAR value for the antenna at the bottom position, as compared to that at the top position. This also agrees with the SAR results shown in Figure 11. These SAR results indicate that

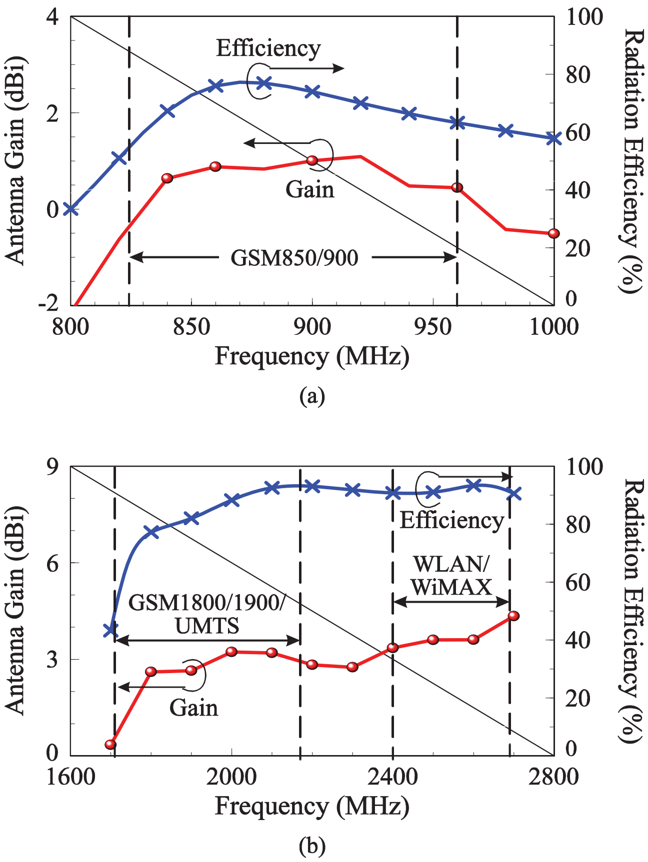

Figure 10 Measured antenna gain and simulated radiation efficiency for the proposed antenna. (a) GSM850/900 band. (b) GSM1800/1900/UMTS/WLAN/WiMAX band. [Color figure can be viewed in the online issue, which is available at www.interscience.wiley.com]

placing the proposed antenna at the bottom position of the mobile phone can result in decreased SAR values for its practical applications in the mobile phone.

4. CONCLUSION

A folded-loop chip antenna capable of seven-band operation covering WWAN/WLAN/WiMAX operation in the mobile phone is presented. The seven-band operation is achieved by introducing a coupling gap into the folded-loop metal pattern embedded inside the FR4 chip base. The presence of the coupling gap not only contributes additional capacitance to compensate for the large imaginary part of the antenna's input impedance but also decreases the real part of the input impedance to be close to 50 Ω, hence resulting in much improved impedance matching for frequencies over the desired lower and upper bands for the proposed antenna. In addition, with seven-band operation obtained, the proposed chip antenna occupies a small volume of $4 \times 5 \times 40$ mm^3 ($0.8\ cm^3$) only, allowing it to be easily applied inside the mobile phone as an internal mobile phone antenna. Good radiation characteristics of the antenna over the operating bands have also been observed. SAR effects of the proposed antenna placed at the top and bottom positions of the mobile phone have also been studied. Results indicate that placing the proposed antenna at the bottom position of the mobile phone can result in decreased SAR values for its practical applications in the mobile phone.

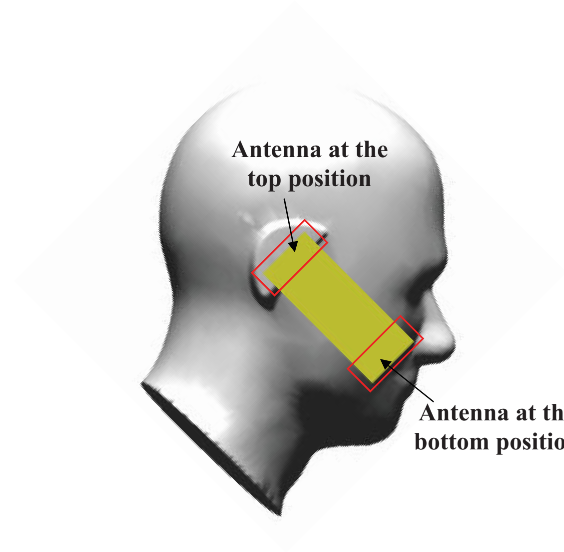

Simulation Model

Simulated SAR Results	925 MHz	1920 MHz
Incident power (dBm)	24	21
Antenna at the top (W/kg)	2.10	2.49
Antenna at the bottom (W/kg)	1.68	1.23
SAR decrease in dB	0.96	3.08

Figure 11 SAR simulation model for the antenna at the top and bottom positions with the head phantom provided by SEMCAD [18] and the simulated SAR results at 925 and 1920 MHz. [Color figure can be viewed in the online issue, which is available at www.interscience.wiley.com]

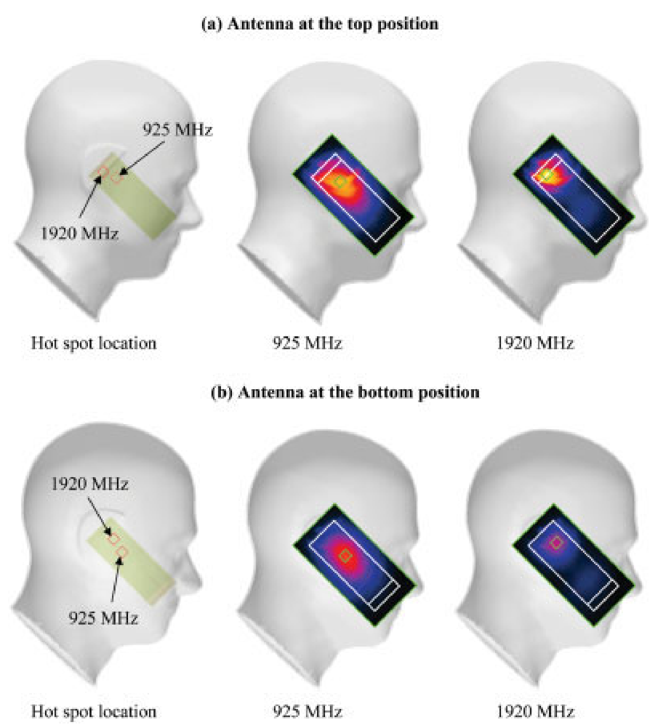

Figure 12 Simulated SAR distributions for the proposed antenna at 925 and 1920 MHz. (a) Antenna at the top position. (b) Antenna at the bottom position. [Color figure can be viewed in the online issue, which is available at www.interscience.wiley.com]

REFERENCES

1. C.I. Lin and K.L. Wong, Internal multiband loop antenna for GSM/ DCS/PCS/ UMTS operation in the small-size mobile phone, Microwave Opt Technol Lett 50 (2008), 1279–1285.
2. C.I. Lin and K.L. Wong, Internal meandered loop antenna for GSM/ DCS/PCS multiband operation in a mobile phone with the user's hand, Microwave Opt Technol Lett 49 (2007), 759–765.
3. B.K. Yu, B. Jung, H.J. Lee, F.J. Harackiewicz, and B. Lee, A folded and bent internal loop antenna for GSM/DCS/PCS operation of mobile handset applications, Microwave Opt Technol Lett 48 (2006), 463–467.
4. B. Jung, H. Rhyu, Y.J. Lee, F.J. Harackiewicz, M.J. Park, and B. Lee, Internal folded loop antenna with tuning notches for GSM/GPS/DCS/ PCS mobile handset applications, Microwave Opt Technol Lett 48 (2006), 1501–1504.
5. C.H. Wu and K.L. Wong, Internal hybrid loop/monopole slot antenna for quad-band operation in the mobile phone, Microwave Opt Technol Lett 50 (2008), 795–801.
6. Y.W. Chi and K.L. Wong, Internal compact dual-band printed loop antenna for mobile phone application, IEEE Trans Antenna Propag 55 (2007), 1457–1462.
7. W.Y. Li and K.L. Wong, Internal printed loop-type mobile phone antenna for penta-band operation, Microwave Opt Technol Lett 49 (2007), 2595–2599.
8. W.Y. Li and K.L. Wong, Surface-mount loop antenna for AMPS/ GSM/DCS/PCS operation in the PDA phone, Microwave Opt Technol Lett 49 (2007), 2250–2254.
9. K.L. Wong, Planar antennas for wireless communications, Wiley, New York, 2003.
10. http://www.wimaxforum.org, Worldwide interoperability for microwave access forum or WiMAX forum.
11. Deployment considerations for fixed wireless access in 2.5 GHz and 3.5 GHz license bands, WiMAX Forum, Available at: http://www.wimaxforum.org/news/downloads/ DeploymentConsiderations White PaperRev 1 4.pdf, 2005.
12. K.L. Wong, Y.C. Lin, and T.C. Tseng, Thin internal GSM/DCS patch antenna for a portable mobile terminal, IEEE Trans Antenna Propag 54 (2006), 238–242.
13. K.L. Wong, Y.C. Lin, and B. Chen, Internal patch antenna with a thin air-layer substrate for GSM/DCS operation in a PDA phone, IEEE Trans Antenna Propag 55 (2007), 1165–1172.
14. O. Kivekas, J. Ollikainen, T. Lehtiniemi, and P. Vainikainen, Bandwidth, SAR, and efficiency of internal mobile phone antennas, IEEE Trans Electromagn Compatib 46 (2004), 71–86.
15. Z. Li and Y. Rahmat-Samii, Optimization of PIFA-IFA combination in handset antenna design, IEEE Trans Antenna Propag 53 (2005), 1770–1777.
16. O. Sotoudeh and T. Wittig, Electromagnetic simulation of mobile phone antenna performance, Microwave J 51 (2008), 78–92.
17. http://www.ansoft.com/products/hf/hfss/, Ansoft Corporation HFSS.
18. http://www.semcad.com, SEMCAD, Schmid & Partner Engineering AG (SPEAG).
19. C.I. Lin and K.L. Wong, Printed monopole slot antenna for internal multiband mobile phone antenna, IEEE Trans Antenna Propag 55 (2007), 3690–3697.

UNIPLANAR COUPLED-FED PRINTED PIFA FOR WWAN OPERATION IN THE LAPTOP COMPUTER

Kin-Lu Wong and Shih-Jia Liao
Department of Electrical Engineering, National Sun Yat-Sen University, Kaohsiung 80424, Taiwan; Corresponding author: liaosj@ema.ee.nsysu.edu.tw

Received 9 June 2008

ABSTRACT: *In this article, a uniplanar printed PIFA (planar inverted-F antenna) with a coupling feed for application as an internal laptop computer antenna for penta-band WWAN (wireless wide area network) operation is presented. The proposed PIFA has a compact structure and can be easily printed on one side of a small 0.8-mm thick FR4 substrate of size 11 × 59 mm², making it very promising to be embedded inside the casing of the laptop computer, especially for the thin-profile laptop computer. With the coplanar coupling feed, the large inductive input reactance of the PIFA at around 900 MHz is compensated, and dual-resonance excitation for the antenna's lower band at about 900 MHz is obtained, which allows it to easily cover GSM850/900 operation. A wide operating band is also achieved for the antenna's upper band at about 1900 MHz, and a bandwidth of larger than 500 MHz is obtained to cover GSM1800/1900/UMTS operation. That is, the proposed PIFA covers all the five operating bands of GSM850/900/1800/1900/UMTS for WWAN operation. Details of the proposed PIFA are presented.* © 2008 Wiley Periodicals, Inc. Microwave Opt Technol Lett 51: 549–554, 2009; Published online in Wiley InterScience (www.interscience.wiley.com). DOI 10.1002/mop.24084

Key words: *internal laptop computer antenna; PIFA; WWAN antenna; multiband operation; coupling feed*

1. INTRODUCTION

The internal WWAN antennas for covering GSM850/900/1800/1900/UMTS (824–894/890–960/1710–1880/1850–1990/1920–2170 MHz) operation are becoming a necessity for many modern laptop computers. By incorporating the internal WWAN antenna and the traditional 2.4/5 GHz internal WLAN (wireless local area network) antenna embedded in the laptop computers [1–6], ubiquitous wireless internet access can be achieved. Some internal WWAN antennas for laptop computer applications have also been reported in the published papers. The recently reported internal WWAN antennas include a dual-band open-loop antenna for GSM900/1800 operation [7] and a quad-band antenna with parasitic elements for GSM850/900/1800/1900 operation [8]. The former design can be printed on a planar structure; however, only two of the five desired operating bands are obtained. The latter design, although four operating bands are obtained, shows a three-dimensional structure and is not promising for the thin-profile laptop computer applications.

A design on combining the GSM900/1800 WWAN and 2.4/5 GHz WLAN internal antennas into a combo antenna with optimized isolation has also been studied [9]. Embedding the WWAN antenna in the USB (universal series bus) dongle for the laptop computer to provide wireless internet access is also a promising alternative [10, 11] for the internal WWAN antenna for the laptop computers. However, these available antenna designs cannot cover all the five desired operating bands of GSM850/900/1800/1900/UMTS for WWAN operation.

In this article, we propose a uniplanar coupled-fed printed PIFA for penta-band WWAN operation in the laptop computer. The proposed PIFA is easily printed on one side of a thin FR4 substrate at low cost and occupies a small area of 11×59 mm², making it